

Supplementary Information for

Dynamics of Amphiphilic Block Copolymers in an Aqueous Solution: Direct Imaging of Micelle Formation and Nanoparticle Encapsulation

Chang Li^{1,2,3}, Che Chen Tho^{1,2,4}, Daria Galaktionova⁵, Xin Chen³, Petr Král^{5,6}, and
Utkur Mirsaidov*^{1,2,4,7,8}

1. Department of Physics, National University of Singapore, 117551, Singapore
2. Centre for BioImaging Sciences and Department of Biological Sciences, National University of Singapore, 117557, Singapore
3. School of Materials Science and Engineering, East China University of Science and Technology, Shanghai 200237, P. R. China
4. Centre for Advanced 2D Materials and Graphene Research Centre, National University of Singapore, 117546, Singapore
5. Department of Chemistry, University of Illinois at Chicago, Chicago, IL 60607, USA
6. Departments of Physics and Biopharmaceutical Sciences, University of Illinois at Chicago, Chicago, IL 60607, USA
7. NUSNNI-NanoCore, National University of Singapore, 117411, Singapore
8. Department of Materials Science and Engineering, National University of Singapore, 117575, Singapore

*Correspondence: mirsaidov@nus.edu.sg

Table of Contents:

1. Identifying core and corona of polymeric micelles	2
2. Additional molecular dynamics simulations results	3
3. Coalescence of polymeric micelles.....	5
4. Encapsulation of gold NPs: <i>ex situ</i> and <i>in situ</i> control experiments.....	5
5. Supplementary movie captions	7
6. Supplementary references	7

1. Identifying core and corona of polymeric micelles

The contrast difference within a polymeric micelle observed in our *in situ* TEM images (Figure 2A-B and S1B), which we attributed to a micellar core (darker contrast) and corona (lighter contrast), is also clearly distinguishable in the micelles formed *ex situ* (Figure S1A). The concentration of polymer solution drop-casted onto the carbon film of a TEM grid for the *ex situ* micelle formation was the same as in *in situ* experiments (7.5 mg/mL).

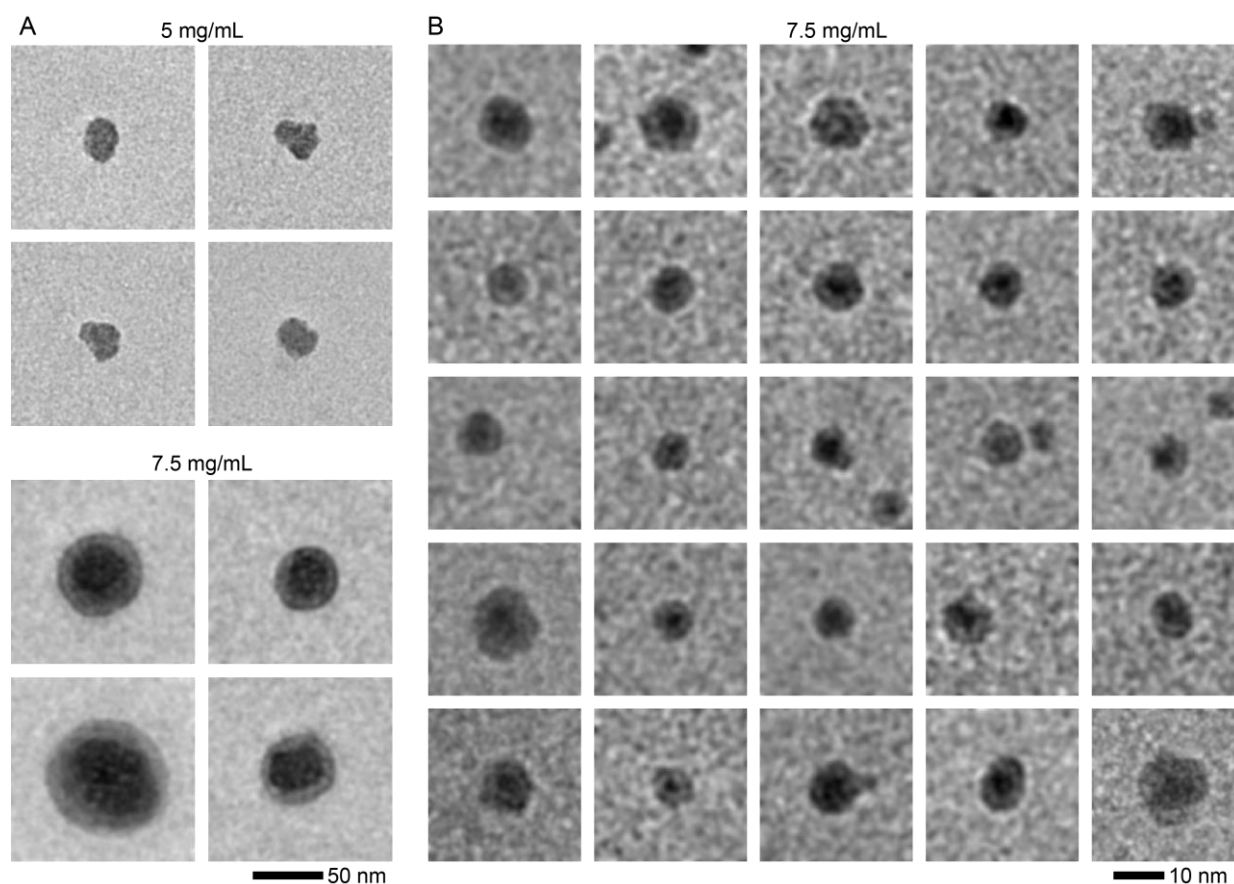


Figure S1. Visualizing the micellar core and corona. (A) TEM images of block copolymer micelles formed *ex situ* after drop-casting 5 mg/mL and 7.5 mg/mL aqueous copolymer solutions onto the carbon film of a TEM grid. At a copolymer concentration of 7.5 mg/mL, these images show darker contrasts in the center and lighter contrast near the edge, which we attribute to micellar core and corona, respectively. Therefore, for our *in situ* TEM experiments, we chose the copolymer concentration to be 7.5 mg/mL. (B) The frames from *in situ* TEM movies of different micelles also show the darker contrast in the centre and lighter contrast near the edge of micelles. The contrast difference in the case of the *in situ* micelles is much weaker compared to the *ex situ* micelles in (A).

We also note that for *in situ* TEM imaging experiments, using a higher block copolymer concentration results in rapid micelle formation that happens faster than we can start imaging (*i.e.*, it takes >5 min before we can start imaging once the solution is prepared; see methods) (Figure S2). The micelles that form in a solution with a higher block copolymer concentration (15 mg/mL) are slightly

bigger than the ones that form at a concentration of 7.5 mg/mL, consistent with earlier cryo-TEM studies.¹

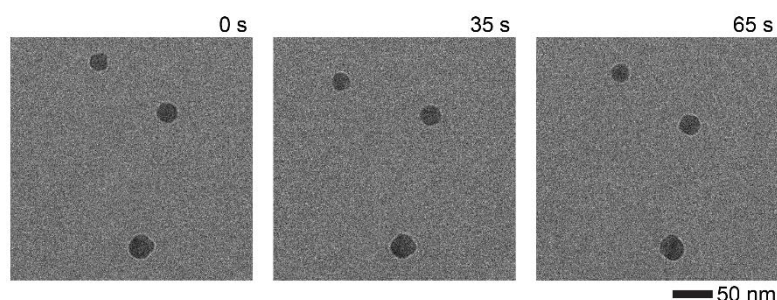


Figure S2. Time series of *in situ* TEM images of micelles in an aqueous solution of block copolymer (15 mg/mL). TEM image series show that at a high block copolymer concentration, micelles form before we can start to acquire movies. Note that there is a delay of > 5 min between preparing the solution and imaging. This delay is associated with the time needed to load the solution into the liquid cell and holder before imaging.

2. Additional molecular dynamics simulations results

In order to test the size dependence of the micelles on the number of comprising monomers, we simulated micelles from 10, 20, and 40 monomers for 20 ns as shown in Figure S3A and Supplementary Movie 4. In each case, the micelle radius has been estimated from the radial density profile according to:

$$r = \sqrt{5/3} r_{\text{gyr}},$$

where r_{gyr} is the average radius of gyration of the micelle, calculated along the simulation trajectories using VMD (Visual Molecular Dynamics) analysis scripts.² A small increase in r_{gyr} of the hydrophobic core from 2.5 nm to 2.7 nm was observed for extra 10 monomers (for micelles from 10 and 20 copolymers, respectively). Much bigger increase of r_{gyr} of the hydrophobic core from 2.7 nm to 3.5 nm was observed for extra 20 monomers (for micelles from 20 and 40 copolymers, respectively). The density profiles of micelles (Figure S3B) were calculated using $\rho = m/V$ for the spherical shells starting from the centre of mass and with a step of 0.1 nm.

To identify the interactions between the polystyrene-capped gold NP and the block copolymers during the NP encapsulation, we plotted the radial density profiles of EO₁₀₀ and PO₆₅ blocks of the copolymer and the polystyrene obtained from our 20-ns-long MD simulation of NP-copolymer system (Figure S4). Large overlap between the radial density profiles of hydrophobic blocks (PO₆₅) and

polystyrene indicates that NP encapsulation is driven by a strong hydrophobic interaction between the capping agent and copolymer.

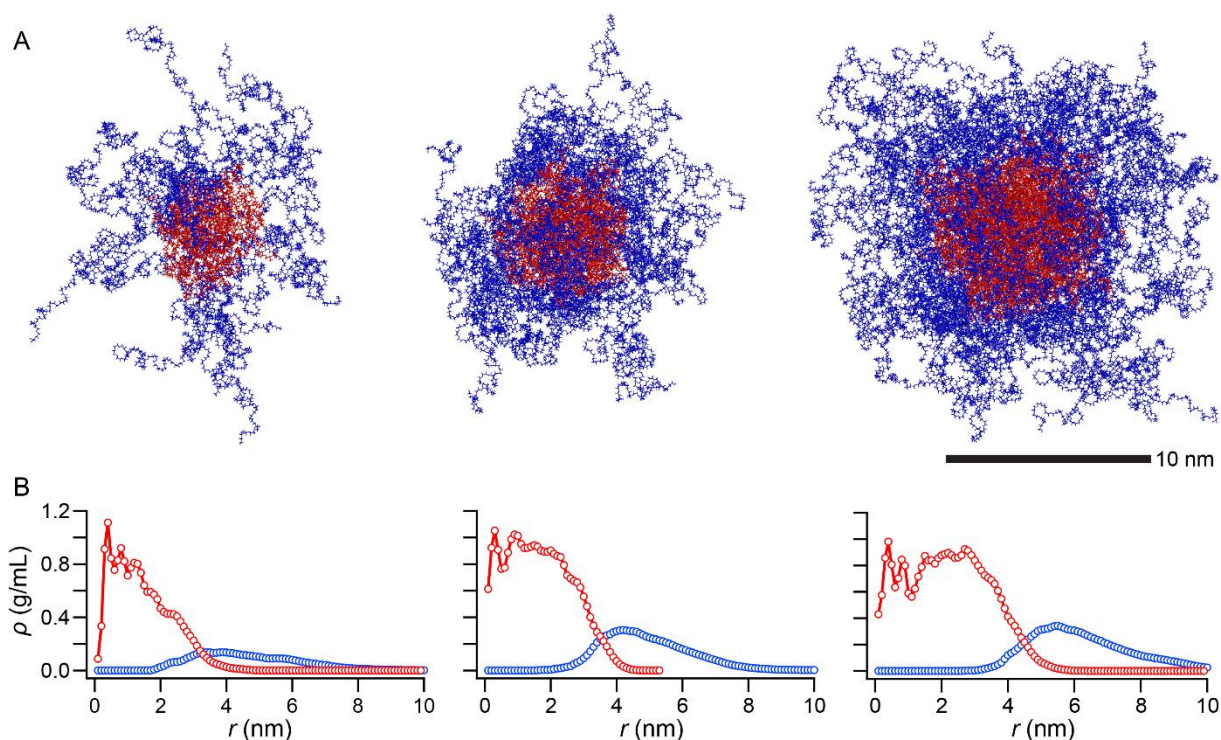


Figure S3. Micelles simulated from different number of copolymers. (A) (Left to right) Micelles from 10, 20, and 40 copolymers (EO₁₀₀-PO₆₅-EO₁₀₀) with the respective overall diameters of ~15 nm, ~15 nm, and ~19 nm. The corresponding diameter of their hydrophobic cores is ~6 nm, ~7 nm, and ~9 nm. (B) Corresponding radial density profiles of the PO (red) and EO (blue) groups for micelles from 10, 20, and 40 block copolymer molecules.

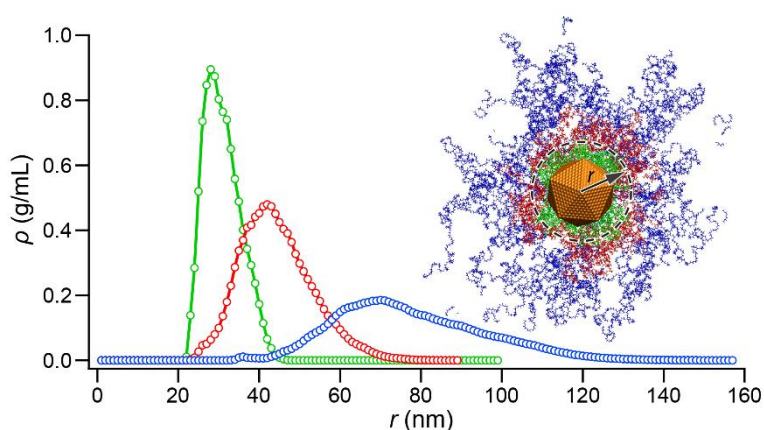


Figure S4. Radial density profile of the capping agent and copolymer blocks. The plot of radial density profile of EO₁₀₀ (blue), PO₆₅ (red) polymer blocks and polystyrene (green). Here, 40 block copolymer molecules (EO₁₀₀-PO₆₅-EO₁₀₀) are adsorbed onto the polystyrene-capped gold NP whose diameter is 5.2 nm. Polystyrene has a large overlap with the PO₆₅ blocks and no overlap with the EO₁₀₀ blocks, which indicates that the NP encapsulation is due to the hydrophobic interaction between the PO₆₅ blocks and polystyrene.

3. Coalescence of polymeric micelles

To examine the possible interactions and coalescence between the micelles, we identified all the micelles that come into direct contact with each other (Figure S5). Out of 174 micelles, only nineteen of them came into contact and only four of them coalesced (*i.e.*, two pairwise coalescence events). Note that in both cases of the coalescence, the micelles only coalesce with very small aggregates (Figure S5A). When the size of micelles are larger, they do not coalesce upon contact (Figure S5B).

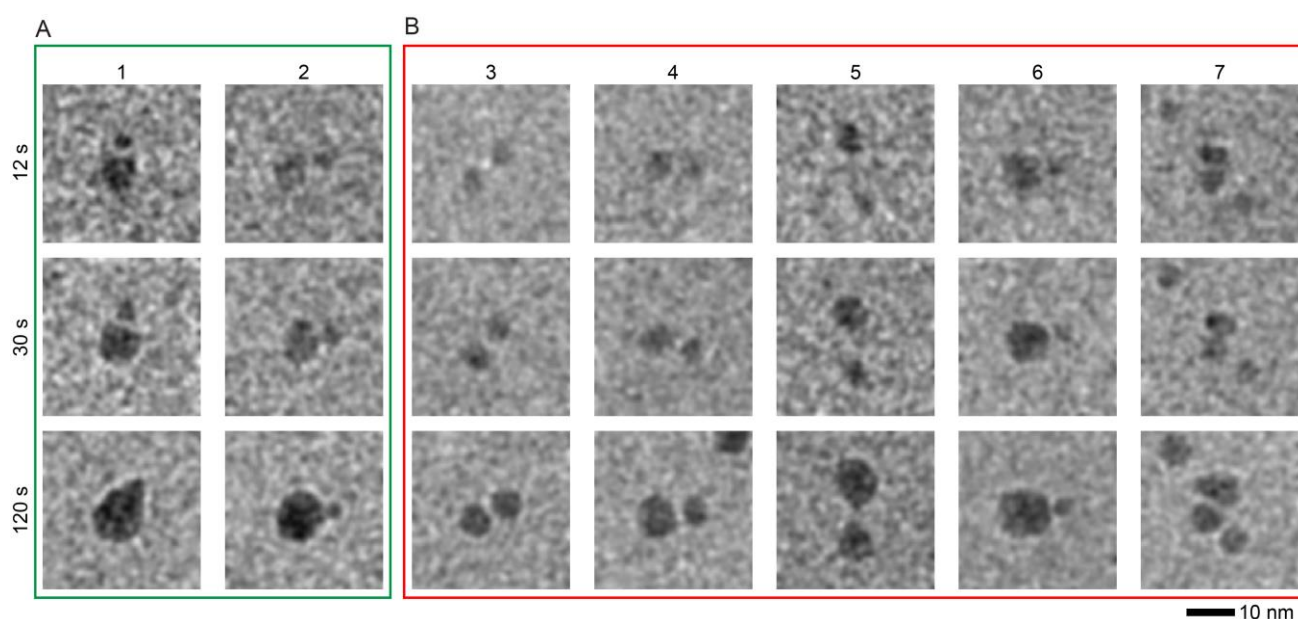


Figure S5. TEM images of micelle-micelle contact. (A) Time series of *in situ* TEM images showing the coalescence between micelles and small aggregates are shown in the green box. (B) Time series of *in situ* TEM images showing the absence of the coalescence upon micelle-micelle contact between large micelles are shown in the red box.

4. Encapsulation of gold NPs: *ex situ* and *in situ* control experiments

This section presents a set of control experiments that were carried out in order to validate the results of NP encapsulation shown in Figure 3 of the main text. Figure S6A shows the TEM images of nine polystyrene-capped (hydrophobic) NPs which are encapsulated with block copolymer shell. The specimen was prepared by mixing the NPs with copolymer solution and drop-casting them onto the carbon film of a TEM grid (*ex situ* experiment). The concentration of the NPs and block copolymers are the same as in our *in situ* experiments (Figure 3A-C): $\sim 3.7 \times 10^{12}$ NPs/mL and 7.5 mg/mL, respectively. In the absence of block copolymers, we did not observe any shell formation in the *ex situ* TEM images (Figure S6B).

In the case of citrate-capped gold NPs at a concentration of $\sim 4.9 \times 10^{11}$ NPs/mL, we did not see any evidence of encapsulation in the presence of copolymers (7.5 mg/mL) in our *ex situ* TEM images (Figure S6C), which is consistent with our *in situ* TEM studies (Figure 3D). Also, no encapsulation was observed in the absence of the block copolymers (Figure S6D).

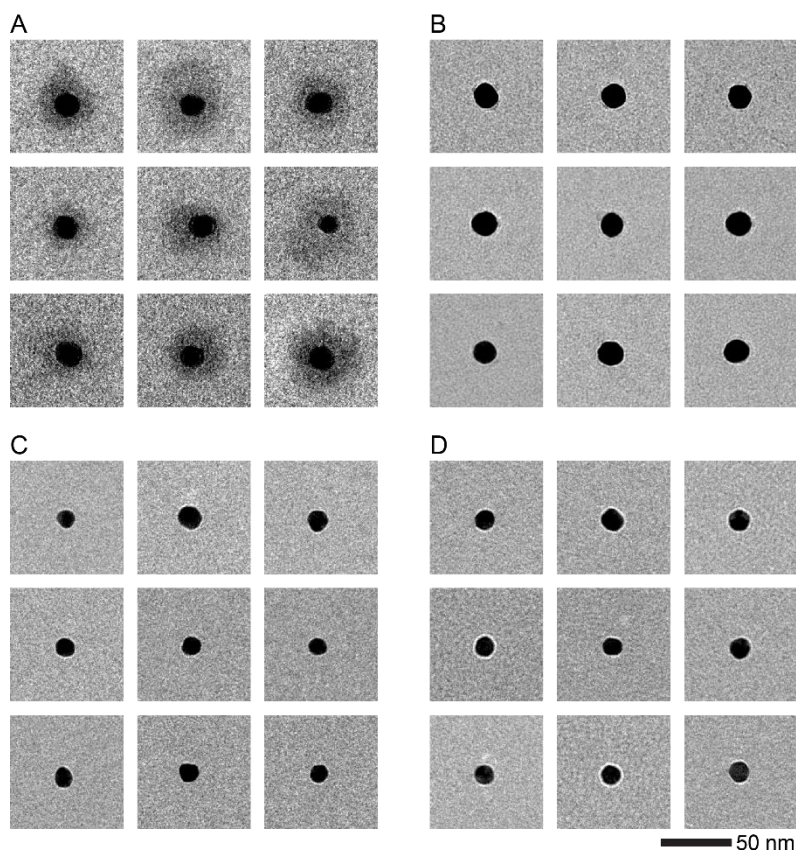


Figure S6. *Ex situ* control experiments of NP encapsulation by block copolymers. (A) TEM images of a drop-casted solution of polystyrene-capped (hydrophobic) gold NPs containing block copolymers (7.5 mg/mL). (B) TEM images of the same polystyrene-capped NPs in the absence of copolymers. (C) TEM images of citrate-capped (hydrophilic) gold NPs in the presence of block copolymers (7.5 mg/mL) in solution. (D) TEM images of citrate-capped (hydrophilic) gold NPs in the absence of copolymers in the solution.

We also tested the effect of block copolymer concentration on NP encapsulation *in situ* and compared it to the results shown in Figure 3, which were obtained with the block copolymer concentration of 7.5 mg/mL. Our results show that at low block copolymer concentration (~ 1.5 mg/mL), there is no detectable encapsulation within 120 s of imaging (Figure S7A). At high concentration (15 mg/mL), block copolymers encapsulate the NPs rapidly; by the time we start imaging ($t = 0$ s), NPs are already encapsulated (Figure S7B).

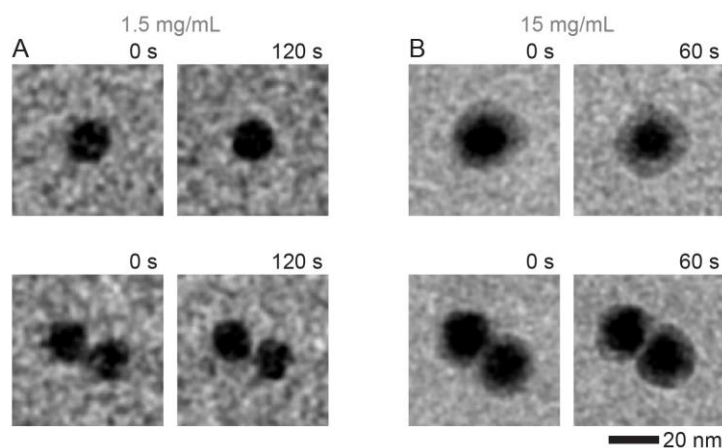


Figure S7. *In situ* TEM imaging of NP encapsulation by block copolymers (control experiments). (A) At block copolymer concentration of 1.5 mg/mL, NPs are not encapsulated by the copolymers. Top and bottom panels show one and two NPs in the solution, respectively. (B) At block copolymer concentration of 15 mg/mL, NPs are encapsulated by the copolymers rapidly (*i.e.*, before we manage to start the imaging). Top and bottom panels show the encapsulation of one and two NPs, respectively.

5. Supplementary movie captions

Movie 1: *In situ* TEM movie showing the nucleation and growth dynamics of micelles in an aqueous solution of EO₁₀₀-PO₆₅-EO₁₀₀ displayed in Figure 1A.

Movie 3: *In situ* TEM movie showing the formation of micelle in an aqueous solution of EO₁₀₀-PO₆₅-EO₁₀₀ displayed in Figure 2A.

Movie 3: *In situ* TEM movie showing the formation of micelle in an aqueous solution of EO₁₀₀-PO₆₅-EO₁₀₀ displayed in Figure 2B.

Movie 4: MD simulation showing the 20-ns dynamics of micelles comprising 10, 20, and 40 EO₁₀₀-PO₆₅-EO₁₀₀ molecules. Water molecules are omitted for clarity.

Movie 5: *In situ* TEM movie showing the encapsulation of polystyrene-capped gold NPs with block copolymers in an aqueous solution displayed in Figure 3A.

Movie 6: MD simulation showing the 20-ns dynamics of polystyrene-capped gold NPs encapsulated with 40 EO₁₀₀-PO₆₅-EO₁₀₀ molecules (Figure 3E). Water molecules are omitted for clarity.

6. Supplementary references

1. Y.-M. Lam, N. Grigorieff and G. Goldbeck-Wood, *Physical Chemistry Chemical Physics*, 1999, **1**, 3331-3334.
2. S. Bogusz, R. M. Venable and R. W. Pastor, *The Journal of Physical Chemistry B*, 2000, **104**, 5462-5470.